Direct Visualization of the Binding of c-Myc/Max Heterodimeric b-HLH-LZ to E-Box Sequences on the hTERT Promoter†

Réjean Lebel, François-Olivier McDuff, Pierre Lavigne, and Michel Grandbois*

Département de pharmacologie, Faculté de médecine et des sciences de la santé, Université de Sherbrooke, Sherbrooke, QC, Canada J1H 5N4

Received January 15, 2007; Revised Manuscript Received May 4, 2007

ABSTRACT: Myc and Max belong to the b-HLH-LZ family of transcription factors. Heterodimerization between Myc and Max or homodimerization of Max allows these proteins to bind their cognate DNA sequence known as the E-box (CACGTG). Recent evidence has suggested that the c-Myc/Max heterodimeric b-HLH-LZ could interact to form a head-to-tail dimer of dimers and induce complex topologies such as loops in promoters containing more than one E-box sequence. In an attempt to shed light on this hypothesis, the interaction between the heterodimeric b-HLH-LZ of c-Myc/Max and a fragment of the hTERT promoter containing two E-box sequences was studied by atomic force microscopy. Specific binding events were observed at both E-box sites with equal probabilities. In accordance with previous results obtained by EMSA, we observed that the specific binding of the c-Myc/Max b-HLH-LZ bends the promoter. However no looping could be observed in a wide range of concentration encompassing the K_a (association constant) of the putative tetramer and the K_a for the specific binding of the heterodimer. In contrast, experiments performed with a mandatory c-Myc/Max b-HLH-LZ tetramer incubated with the hTERT promoter fragment allowed for the visualization of loops and cross-linked DNA strands originating from specific binding. Altogether, our results indicate that the c-Myc/Max b-HLH-LZ dimer binds specifically and equally to both E-box sites of the hTERT promoter and induces a significant bending of the promoter and that the suggested oligomerization of the c-Myc/Max heterodimeric b-HLH-LZ, if existing, is most likely too weak to induce the formation of a loop in a promoter.

Transcription factors bind specific DNA sequences in promoters to regulate the transcription of genes. The accurate localization of their specific binding sites is crucial to the understanding of the mechanisms involved in activation and repression of gene transcription. Interestingly, some transcription factors are reported to have the ability to loop promoters as part of their regulation mechanism (*1*). Indeed, looping has been proposed to influence the sensitivity of promoters to transcription factor levels, to reduce transcriptional noise, to allow cooperative binding of multiple sites, and also to impose topological constraints that could significantly affect DNA binding and gene regulation by other transcription factors (*2*).

c-Myc and Max are members of the Myc/Max/Mad network of b-HLH-LZ transcription factors. This network is central to the control of cell growth and proliferation (*3*, *4*). The HLH and the LZ domains are essential to the dimerization of these proteins and the b-regions essential to their association with specific DNA sequences (*5*). The Max protein can dimerize (Max/Max homodimer) and bind E-box sequences "CACGTG" (*5*). However, the proteins from the Myc and Mad families cannot homodimerize and rely on Max to heterodimerize and bind E-box sequences in the promoter of target genes (*3*, *4*). As a heterodimer with Max, c-Myc can activate the transcription of growth and proliferation (*3*). Activation of transcription by c-Myc is associated with the recruitment of coactivators with histone acetyl transferase activity (*3*). Because Max is lacking specialized domains capable of recruiting coactivator or corepressors, its role was proposed to be limited to the competition for identical binding sites as a homodimer and partnership to other bHLH-LZ proteins that cannot homodimerize (*5*). As a heterodimer with Max, the Mad protein antagonizes c-Myc by competing for Max and recruiting corepressors with histone deacetylase activity to target gene promoters (*4*).

The solution structure of the homodimeric b-HLH-LZ of Max/Max free of DNA has been solved (*7*) and the crystal structures of the Max/Max (*8*, *9*), Mad1/Max and c-Myc/Max (*10*) b-HLH-LZ bound to an E-Box have also been determined. In the latter case, the heterodimeric c-Myc/Max b-HLH-LZ (cross-linked by the C-termini) bound to DNA packs as a head-to-tail dimer of dimers in its crystalline form (*10*). In the absence of DNA, this cross-linked dimer is reported to sediment as a dissociable species with a molecular weight corresponding to a tetramer. This has led to the hypothesis that the functional form of the c-Myc/Max heterodimer is a dimer of dimers. Moreover, it was proposed that this head-to-tail tetramer could loop promoters containing more than one E-box. Looping was also proposed to be an integral component of the mechanism of the c-Myc transcriptional activities. Verification of this hypothesis is

† This research was funded by grants of the Canadian Institutes of Health Research (CIHR) (P.L., M.G.) and the Natural Sciences and Engineering Research Council of Canada (NSERC) (M.G.). P.L. is a Junior 2 scholar of the Fonds de la Recherche en Santé du Québec (FRSQ), and M.G. holds a Canada Research Chair (CRC).

* All correspondence should be addressed to Michel Grandbois, Département de pharmacologie, Faculté de médecine et des sciences de la santé, Université de Sherbrooke, 3001 12e avenue nord Sherbrooke, Québec, Canada J1H 5N4. Tel: 819-820-6868 ext 12369. Fax: 819-564-5400. E-mail: Michel.Grandbois@usherbrooke.ca.

10.1021/bi700076m CCC: $37.00
Published on Web 08/17/2007

of tremendous importance for our understanding of c-Myc activities. Experimental approaches that allow for the direct observation of protein/DNA interactions and topological changes are necessary. Atomic force microscopy (AFM) qualifies as such an approach. Indeed, recent work by Lysetska et al. (2005) with the ORF80 protein demonstrates that even a small protein (9.5 kDa) can be visualized on its cognate DNA sequence (*11*), and that two binding sites as close as 60 bp apart can be resolved. This study also allowed determining the identity of the binding site of ORF80 and the oligomeric state of this transcription factor as well as topological changes induced on a target promoter. Other DNA binding/processing proteins also have been successfully studied using AFM: MutS (*12*), *Eco*KI (*13*), RNA polymerase from *Escherichia coli* (*14*−*16*), RecA (*17*), *Eco*P15I (*18*), Pho4b (*19*), c-Myb-C and C/EBPβ (*20*), p53 (*21*), and histones/nucleosomes (*22*).

To observe loop structures formed by a potential c-Myc/Max b-HLH-LZ dimer of dimers, we used a region of the promoter of human telomerase reverse transcriptase gene (phTERT) which is well-known to be regulated by c-Myc (*3*). This region of the promoter contains two E-box sequences that allow for the simultaneous binding of two c-Myc/Max b-HLH-LZ heterodimers. Specifically, our goals were to observe the specific binding of the heterodimeric c-Myc/Max b-HLH-LZ onto phTERT, and to directly evaluate the impact of this interaction on the topology of DNA in physiological conditions through AFM imaging and electrophoretic mobility shift assays (EMSA). We were able to unveil the specific interactions by the statistical analysis of the location of binding events on phTERT. We also report that the specific binding induces a bend in the promoter region studied. However, no specific loop structure (or cross-link) was observed at concentration near the K_d (dissociation constant) of b-HLH-LZ/E-box interaction. To ascertain the oligomeric state of the c-Myc/Max complex, an EMSA was performed, confirming the absence of any tetrameric entity under the conditions used. Conversely, an artificial mandatory tetramer of the c-Myc/Max b-HLH-LZ allowed for the formation and observation of loops and cross-links of the phTERT sequence.

MATERIALS AND METHODS

DNA Substrate. A 1814 bp long DNA fragment was amplified by PCR from outside the multicloning site of a pGL2-basic plasmid containing an insert of phTERT (−1250 to +394) (kindly provided by Sylvia Bacchetti (*23*)). The PCR product was loaded on a 1% agarose gel, and the specific band was extracted with the QIAGEN kit and protocol. DNA substrate solutions obtained were characterized by spectroscopy and diluted to 50 nM in 10 mM Tris-HCl 1 mM EDTA, pH 8 (TE).

Expression and Purification of the b-HLH-LZs of c-Myc and Max. A pET3a vector containing the cDNA sequence coding for the c-Myc b-HLH-LZ (aa 353 to 436) plus a GSGC C-terminal tail was transformed in *E. coli* BL21 Codon + (Novagen). For clarity this construct will be referred to as c-Myc* in the rest of the text. Single colonies were picked and grown overnight as precultures of 10 mL of LB medium. Then, 1 L of LB medium was inoculated. The culture was incubated at 37 °C until the $OD_{595\ nm}$ reached 0.6. Protein expression was induced overnight at 37 °C by adding IPTG (0.6 mM). Cells were harvested by centrifugation at 3500*g* and frozen at −20 °C until purification. Bacteria were lysed in 10 mL of a buffer containing 50 mM HEPES-NaOH (pH 7.5), 100 mM NaCl, 10 mM $MgCl_2$, 5 mM DTT, 0.35 mg/mL lysozyme, and incubated for 30 min at 37 °C. Triton X-100 was added to the solution to obtain a final concentration of 1%, and then cells were homogenized by sonication on ice. DNAase I (0.04 mg/mL) was added and the solution was incubated at 37 °C for 60 min. Inclusion bodies were collected by centrifugation at 30000*g* for 30 min at 4 °C and resuspended with 15 mL of a buffer containing 6 M urea, 100 mM sodium acetate (pH 5.0), 0.5 M GuHCl, and 25 mM DTT. After solubilization, 15 mL of 2 M urea was added to dilute the solution, followed by a centrifugation at 30000*g* for 30 min at 4 °C. Supernatant was loaded on a HiTrap SP HP column (GE Healthcare) preconditioned with buffer A (50 mM sodium acetate (pH 5.0)). The column was washed with 5 volumes of a buffer containing 4 M urea, 50 mM Tris-HCl (pH 7.5). Elution of c-Myc was performed with a gradient (25 mM/mL) from 0% to 100% of buffer B (buffer A with 5 M NaCl). The b-HLH-LZ of Max (aa 22 to 104 plus the GSGC C-terminal tail) was expressed and purified as described elsewhere (*24*). This construct will be referred to as Max* in the rest of the text.

Preparation of Protein Samples. In solution, Max* forms a stable and dissociable dimer at room temperature (*24*−*27*). However, in the presence of c-Myc*, it preferentially and reversibly assembles as a heterodimer, while c-Myc* does not appreciably homodimerize (*25*−*27*). The reported K_d for the Max* homodimer and c-Myc/Max homodimer are approximately 600 nM and 100 nM respectively (*25*−*27*). The cysteines located at their C-termini will be either kept in a reduced state by adding DTT (10 mM) in solution or cross-linked by air-oxidation at pH 8.8 in the presence of 30 mM of Cu^{++} ($CuSO_4$) in a Tris-HCl buffer (100 mM) containing 6 M GuHCl overnight followed by a buffer exchange. The covalent Max*/Max* and c-Myc*/c-Myc* were formed accordingly. The covalent c-Myc*/Max* heterodimer was generated through oxidation of an equimolar mixture of Max* and c-Myc*, and by further purifying the mixture by HPLC on a homemade reverse-phase C12 column using a gradient of acetonitrile dissolved in water using trifluoroacetic acid as a counterion (to isolate the heterodimer from the homodimers formed). The mandatory c-Myc*/Max* tetramer was obtained by mixing an equimolar ratio of c-Myc*/c-Myc* and Max*/Max*.

Electrophoretic Mobility Shift Assays (EMSA). The dsDNA was annealed by heating oligonucleotides containing E-box sequence (underlined) 5′-d(CCCCCAACACGTGTTGCCTGA)-3′ and 5′-d(TCAGGCAACACGTGTTGGGGG)-3′ at 90 °C and cooling the solution slowly to room temperature. All complexes were obtained by incubating 15 μM proteins in dimer units with 15 μM dsDNA, at room temperature for 20 min in 20 mM Tris-HCl (pH 8.0) and 50 mM KCl. For the DNA complexes with dissociable Max*/Max* and c-Myc*/Max*, 10 mM DTT was added. The complexes were loaded on a polyacrylamide gel (6% in a 1X Tris-acetate buffer; 40 mM Tris, 20 mM acetic acid) and run in 1 X TBE at 100 V. The gels were stained in ethidium bromide and visualized under UV light to reveal the DNA and DNA−protein complexes.

Cationic PAGE, His-HEPES-KOH. The conditions for the cationic electrophoresis were adapted from the work of Chrambach and Jovin (*28*). In more detail, free base histidine was used as the trailing ion and potassium hydroxide as the leading ion, in a HEPES buffer. A 4% acrylamide bis-

acrylamide (29:1) stacking gel (125 mM HEPES-KOH, pH 7.7, 6 M urea) and a 12% acrylamide bis-acrylamide (29:1) resolving gel (375 mM HEPES-KOH, pH 7.0, 6 M urea) were used. The anode buffer was made of 25 mM HEPES and 175 mM histidine free base, and the cathode buffer was composed of 200 mM HEPES-KOH (pH 7.0). Loading buffer (62.5 mM HEPES-KOH (pH 7.7), 30% glycerine, and 6 M urea) was added to the samples with a ratio of 1:1. Horse heart cytochrome C was used to follow the migration. Polarity was inverted, and the migration was conducted at 200 V and 18 mA for 2 h.

Circular Dichroism Spectropolarimetry. Circular dichroism measurements were performed on a Jasco J-810 spectropolarimeter equipped with a Jasco Peltier-type thermostat. The instrument was calibrated with an aqueous solution of d-10-(+)-camphor-sulfonic acid at 290.5 nm. Samples were loaded into quartz cells (path length of 0.1 cm). Far-UV CD spectra were recorded at the desired temperature from 200 to 250 nm by averaging three scans at 0.1 nm intervals. Sample of proteins from the stock solutions were diluted to the desired concentration in 50 mM KH_2PO_4 (pH 6.8), 50 mM KCl. Before measurement, the samples were incubated for 24 h at room temperature to ensure equilibrium.

Preparation of Samples for AFM Imaging. DNA Samples without Protein. A stock solution of the phTERT was diluted in Tris-acetate buffer to a final concentration of 2 nM DNA, 10 mM Tris-acetate (pH 7.0), and 10 mM $MgCl_2$. *Protein−DNA Samples.* Proteins were incubated with DNA for 30 min in Tris-acetate buffer at a final concentration of 2 nM DNA, 20 to 100 nM protein (dimer units), 10 mM Tris-acetate (pH 7.0), and 10 mM $MgCl_2$. $MgCl_2$ was added in all the buffers as it was found to be the best divalent cation to promote the DNA adsorption onto the mica surface (*30*). Considering the reported K_d for the heterodimer (see above) and the K_d of the E-box complex (90 nM (*25*)), our conditions are adequate to expect specific binding of the c-Myc/Max b-HLH-LZ. Because the bHLH-LZ constructs contained a cysteine at their C-termini, experiments were conducted in the presence of DTT unless cross-linking was desired. AFM imaging performed at a higher concentration of dimer (200 nM) was not suitable for AFM analysis due to extensive coating of the mica surface. Ten microliters of the samples to be imaged was applied on a freshly cleaved mica surface and incubated at RT for 3 min before being washed with 3 mL of deionized water. Finally, the surface was gently dried under argon. Protein−DNA complexes can be firmly attached to the mica substrate as reported in several studies using similar immobilization protocols (*12*−*19*). We observed that dimers were stably bound to the DNA since it was impossible to displace the bound complexes even after extensive washing. In the eventuality of a hypothetical tetramer dissociation into dimeric units, each dimer should remain associated to its respective DNA site, because the dimer−DNA complex is kinetically very stable with a K_{off} of 0.0013 s^{-1} (*29*). This ensures that the dimers remain in close proximity on the mica surface, and the topological constraints associated with these events in DNA strands (loops and cross-links) will be indicative of the occurrence of the putative c-Myc*/Max* tetrameric complex.

AFM Imaging and Analysis. All AFM measurements were performed in tapping mode, in air, with a bioscope (Digital Instruments, Santa Barbara, CA). RTESP7 tips (Veeco Probes, Santa Barbara, CA) were oscillated near their resonance frequency (~300 kHz), and minimal force was applied on the sample (1 V amplitude oscillation, setpoint lowered by small increments until clear images were obtained). All scans were performed at rates varying between 512 and 1024 pixels/s (1 to 2 lines/s), and resolution was kept above 170^2 pixels/μm^2. All image flattening and rescaling were made using the WSxM software (WSxM; http://www.nanotec.es), while lengths, distances, and angles were measured with the Image J software (National Institutes of Health, U.S.A.; http://rsb.info.nih.gov.ij). Each DNA length and distance was manually traced five times with the program, and the values were averaged. The length is taken to be the shortest path from one end to the other, skipping loops into the strand. In such an approach, the presence of a specific loop is detected as a shorter DNA strand population. The protein binding events on the phTERT fragment were measured similarly. Each event accounted for a single N, but yielded two reciprocal distances (one from each end of the DNA fragment), which were plotted together.

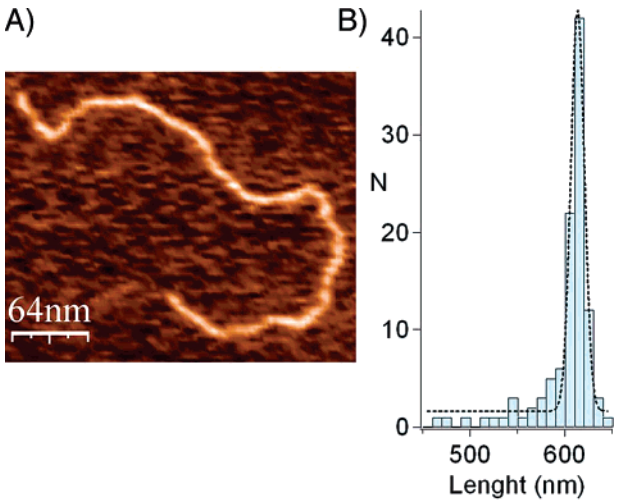

FIGURE 1: Imaging of the phTERT fragment in absence of protein. (A) A phTERT strand on the mica surface imaged by AFM. (B) Length of the DNA strands in absence of protein. Gaussian fit results are reported in Table 1.

RESULTS AND DISCUSSION

Measurement of the Length of the phTERT Fragment. Initially, the average length of the phTERT fragment was assessed. Only strands totally included in the scan area and free of contact with other strands were considered for this measurement (Figure 1A). Figure 1B shows the histogram of the lengths obtained as described in Materials and Methods. The measured length of the DNA strand obtained (613 ± 10 nm, $N = 119$) is close to the 616 nm value expected for a 1814 bp long ds B-DNA (0.34 nm/bp). This indicates that the surface−DNA interactions do not alter the conformation of DNA. This point is particularly important as the overall length of the DNA strands is used to detect the presence of loops and the position of the binding sites. It also indicates that the AFM images performed on the mica surface reflect the DNA conformation in solution prior to its adsorption. The accuracy of the length determination procedure is estimated at ±10 nm from the standard deviation of the Gaussian fits.

Binding of the c-Myc/Max* Heterodimer to phTERT.* As described above, the concentrations of DNA and proteins used are close to or above the K_d of the heterodimeric c-Myc/Max b-HLH-LZ and of its complex with an E-box sequence

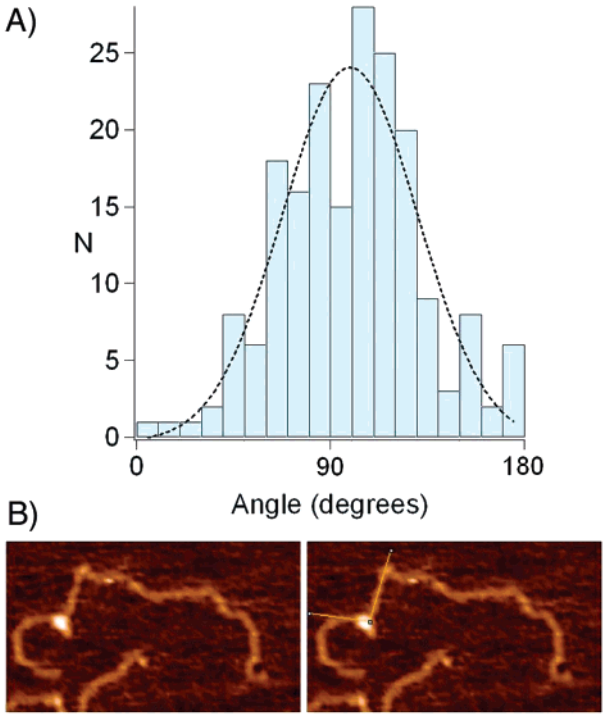

FIGURE 2: The binding of c-Myc*/Max* causes a bend into the promoter. (A) The measured angle of the bend (99° ± 40°) is the reciprocal of the angle caused into the strand. (B) Example of an angle measurement (yellow lines).

ensuring the existence of specific binding events. The binding of c-Myc*/Max* to phTERT fragments is visualized by AFM as small globular objects, on specific location of the DNA strands (Figure 2). Interestingly, as one can observe, the binding of c-Myc*/Max* induces bends in DNA, which were quantified by measuring angles at the protein binding locations. An average angle of 100° (±40°) was obtained, which corresponds to bending a linear strand with a reciprocal angle of 80° (Figure 2A). This result is in good agreement with the previously measured bending angle (74°−82°) of a 120 bp probe caused by the binding of a dimeric b-HLH-LZ (*31*) by EMSA. However, the crystal structures of the b-HLH-LZs bound to E-box sequences (*8*, *10*) revealed no appreciable deviation from the B-form of DNA. This suggests that the conformational change leading to DNA bending originates from the binding event but is transmitted away from the interaction site. This could be due to the restricting effect of the crystal packing forces, or could suggest that long range interactions are responsible for the observed bending of the promoter. Since c-Myc* and Max* bear an excess of positive charge (*Z*), $Z_{c-Myc'SH(pH7.00)} = 7.15$ and $Z_{Max'SH(pH7.00)} = 4.51$, respectively, it is possible that DNA charge screening takes place causing the promoter to bend toward the protein complex. Additionally, it is reasonable to speculate that the formation of an angle from the site of interaction could be the first step toward the formation of a loop in a promoter or more complex topologies by other transcription factors or histones, since such an angle would reduce the necessary energy for the formation of loops or other specific conformations.

The assessment of the specificity of binding of c-Myc*/Max* to the E-box sites was based on the schematized phTERT fragment presented in Figure 3. As previously stated, the selected phTERT fragment contains two E-boxes. Because the identity of each end of the DNA strand cannot

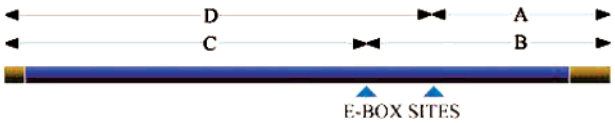

FIGURE 3: phTERT fragment used in AFM imaging experiments. Outer segments (yellow) are located in the plasmid while the inner (blue) segment is the selected phTERT region. Each E-box (blue arrows) yields two possible locations (from each end of the molecule). The four possible measurable lengths are labeled from *A* to *D*. The theoretical distances have been reported in Table 1.

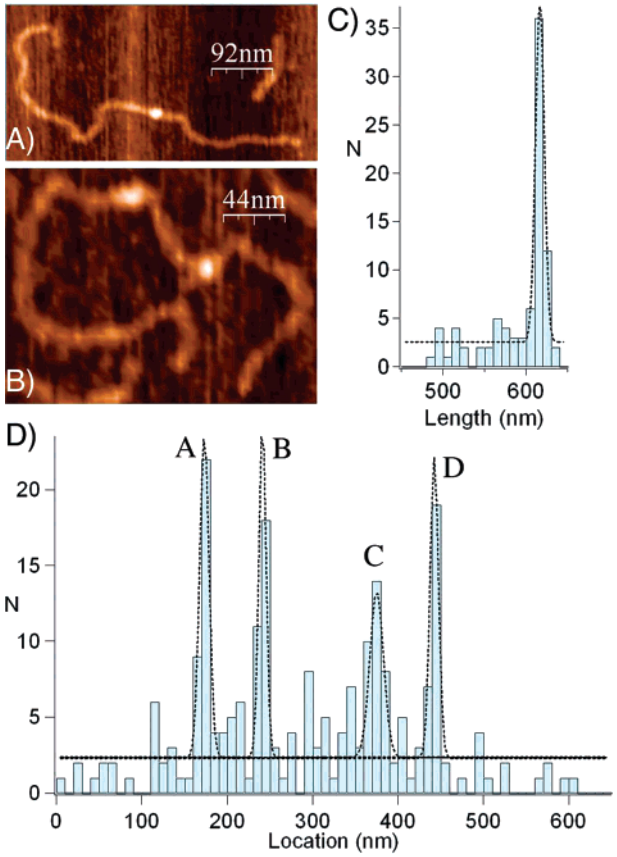

FIGURE 4: Binding of the dissociable c-Myc*/Max* heterodimer to E-boxes on phTERT. Images of a phTERT strand bound by (A) one or (B) two heterodimers. (C) Histogram showing the length of phTERT strands bound by the heterodimer. (D) Histogram showing the position of the heterodimer on the phTERT fragments. Each peak corresponds to a theoretical position labeled from A to D. All Gaussian fits results are reported in Table 1. The four Gaussian fits superimpose at their baselines which correspond to the occurence of unspecific binding events.

be differentiated by AFM, one must measure the two reciprocal DNA-end/binding event distances. Hence, each E-box yields two distances which sum to the full length ($A + D = B + C = L$, the full length of the molecule, Figure 3). Validation of the specific binding sites is carried through a statistical analysis of the binding events along the strand, and comparison against the expected location. A specific loop between E-boxes with a length *E* would decrease the shortest end-to-end distance to a new length L' (where $L' = L - E$). Binding events on a single (Figure 4A) or both (Figure 4B) E-box sites were observed, but the specific double binding event was slightly less frequent. In our experimental design, it was necessary to generate more single than double binding events. Assuming that the hypothetical tetramer exists in solution, a high concentration would cause the tetrameric complexes to occupy both E-box sites, thus preventing the

Table 1: Theoretical and Experimental DNA Strand Length and E-Box Locations[a]

experiment	DNA length (nm)	*A* (nm)	*B* (nm)	*C* (nm)	*D* (nm)
expected	617 546[b]	175	246	370	441
heterodimer[c]	616 ± 8	172 ± 7	241 ± 6	374 ± 11	442 ± 6
tetramer*	614 ± 11 538 ± 8[b]	168 ± 16	240 ± 12	373 ± 18	439 ± 26
homodimer[d]	616 ± 8	173 ± 9	243 ± 7	373 ± 9	442 ± 11
no protein	613 ± 10				

[a] Theoretical distances are calculated based on B-DNA dimensions (0.34 nm/bp). Distances labeled from *A* to *D* (see Figure 3). [b] phTERT fragment looped between its E-boxes. [c] Refers to the dissociable c-Myc*/Max* heterodimer. [d] Refers to the dissociable Max*/Max* homodimer.

formation of loops or cross-links in the DNA strands. For this reason, we used protein/DNA ratios and concentrations in a range generating more single binding events.

The location of the binding events on phTERT were extracted from Gaussian fits of the four peaks present in the histogram (Figure 4D) and corresponded to the expected positions of the E-box sites. For example, the distance *D* which is measured from the 5′ end of the promoter region to the second E-box site theoretically gives 441 nm and was experimentally determined to be 442 ± 6 nm. All values have been reported in Table 1. Because all expected values are within a single standard deviation from the obtained location, it can be assumed that the method employed here is very accurate to localize the E-box sequences in the phTERT fragment through the specific binding of the c-Myc*/Max* dimer. It should also be noted that the area under the localization peaks of each E-box (A and D, B and C) are similar, which can be expected from sites of equal affinity. Importantly, no other complex topologies such as cross-linked DNA strands or loops within single strands were observed. The formation of such topologies are expected if c-Myc*/Max* dimers are to form head-to-tail dimer of dimers as previously proposed (*10*). In this context the observation of two binding events on a single DNA strand (Figure 4A) is particularly interesting since two c-Myc*/Max* dimers associated with a single hTERT strand correspond to a local concentration of the dimer estimated at 2 μM, a concentration well above the proposed K_d for dimer to dimer head-to-tail association (*10*). To estimate this concentration, we have assumed a sphere with a diameter of 71 nm, the distance between the two E-box sites. In these conditions one should confidently expect the formation of a loop in the DNA strand. However such looping was never observed in our conditions despite the fact that more than one hundred AFM micrographs were analyzed. This result is consistent with another study probing the heterodimerization of dissociable c-Myc and Max b-HLH-LZ by fluorescence anisotropy. Indeed, at concentrations above the reported K_d of the head-to-tail dimer of cross-linked heterodimers the anisotropy measured was consistent with that of a dimer (*25*).

Alternatively we have evaluated the length of the DNA fragments in presence of the c-Myc*/Max* complexes in order to indirectly detect the formation of loops. Here we posit that the formation of a loop would reduce the length of the strand by approximately 71 nm, i.e., the distance between the two E-box sites. For this analysis only strands bound by at least one c-Myc*/Max* complex were considered. A length of 616 ± 9 nm ($n = 129$) was obtained (Figure 4C), which corresponds to the expected length (617 nm) of a single hTERT strand, again indicating that no specific loop forms and that the binding of c-Myc*/Max* has little effect on the contour length of DNA. This is also in agreement with the experimentally measured contour lengths of the DNA only (Figure 1). To further investigate concentration effects on the possible formation of loop structures and cross-linked hTERT strand by c-Myc*/Max*, attempts were made to increase the dimer concentrations in solution to 200 nM. AFM images resulting from these experiments were at best ambiguous, indeed the surfaces became extensively coated with proteins and, as a result, very few isolated DNA strands were found uniformly adsorbed on the mica surface. Therefore, to ascertain the oligomeric state of the dissociable heterodimer in the presence of DNA, EMSA were performed.

The Oligomeric State of c-Myc/Max* and the Formation of a Mandatory c-Myc*/Max* Tetramer.* It has been observed that the cross-linked version (C-termini of the LZ) of the heterodimeric b-HLH-LZ bound to DNA packs as a head-to-tail dimer of dimers in the crystalline form (*10*). In absence of DNA, this cross-linked dimer apparently sediments as a dissociable species. In order to ascertain the oligomeric state of the dissociable c-Myc*/Max* heterodimer in the presence of DNA, an EMSA was carried out. This assay was done with the premise that if the dissociable heterodimer associates as a heterotetramer, it will form a stable complex with an E-box probe and shift it with the apparent MW of a tetramer. In contrast, if the dissociable c-Myc*/Max* exists only as a heterodimer, it should modify the electrophoretic mobility of an E-box probe with an apparent molecular weight similar to that of the Max*/Max* dimer, which is a *bona fide* dimer (Figure 5A, lanes 2 and 3). Note that the dissociable and cross-linked c-Myc*/Max* heterodimers form complexes with the E-box with a slightly higher apparent MW (lane 4 and 5) than the Max*/Max*/E-box complexes. This slightly higher apparent molecular weight of the heterodimeric complexes does not correspond to a tetrameric molecular weight, but to an intrinsic difference of the overall charge ($Z_{c-Myc(pH7.00)} = 7.15$ vs $Z_{Max(pH7.00)} = 4.51$), thus a change in electrophoretic mobility. This assertion is validated in Figure 6 where the electrophoretic mobility of covalent c-Myc*/c-Myc* and Max*/Max* dimers in urea and in the absence of SDS is displayed. Here, the electrophoresis was run in a reverse electric field leading to a cationic migration. One can see that the covalent c-Myc*/c-Myc* complex has a larger electrophoretic mobility than that of the covalent Max*/Max* complex, as expected from the higher density of positive charges on c-Myc*. Therefore, since the overall structure of all dimeric complexes is expected to be similar, one can rationalize the lesser electrophoretic mobility of the heterodimeric DNA complexes on the basis of a lesser negative charge density rather than on a MW or oligomeric state difference. We further demonstrate this point with the electrophoretic mobility measurement of a mandatory c-Myc*/Max* tetramer/E-box complex (Figure 5A, lane 6).

The overall structure and assembly of the tetramer are described in Figure 5. In Figure 5B, we present the far UV, CD spectra of c-Myc*/c-Myc*, Max*/Max*, and the mixture

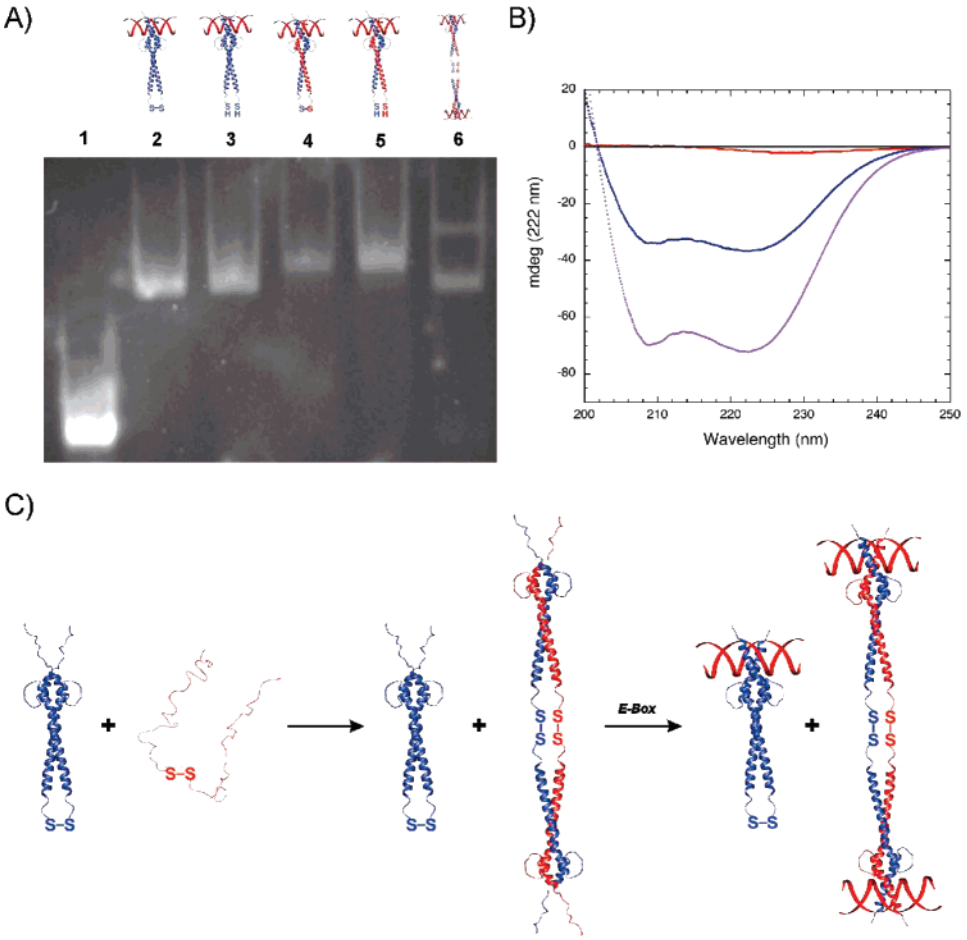

FIGURE 5: Characterization of the oligomeric state of c-Myc*/Max* by EMSA and circular dicroism. Max* is depicted in blue and c-Myc* in red. (A) Lane 1. Free double-stranded E-box DNA. Lane 2. Covalent Max*/Max* homodimer and E-box DNA. Lane 3. Dissociable Max*/Max* homodimer and E-box DNA. Lane 4. Covalent c-Myc*/Max* heterodimer and E-box DNA. Lane 5. Dissociable c-Myc*/Max* heterodimer and E-box DNA. Lane 6 shows two DNA complexes resulting from the incubation of equimolar quantities of covalent c-Myc*/c-Myc* and covalent Max*/Max* (tetramer*) in the presence of E-box DNA. All complexes were formed at a total protein concentration of 0.5 μM protein with an equimolar concentration of double-stranded E-box DNA. (B) Far UV-CD spectra of covalent c-Myc*/c-Myc* (red,), covalent Max*/Max* (blue), and the mixture of covalent c-Myc*/c-Myc* and Max*/Max* (purple/tetramer*) recorded at pH 6.8 and 20 °C at 16, 32, and 64 μM in total concentration (monomeric units) respectively. (C) Sketch describing the formation of the mandatory c-Myc*/Max* heterotetramer (tetramer*) and its complex with an E-box probe. Note that the covalent c-Myc*/c-Myc* do not exist as a folded b-HLH-LZ in the absence or in the presence of E-box sequences. Both the tetramer* and covalent Max* homodimer are present and form their corresponding DNA complexes, while the covalent c-Myc*/c-Myc* dimer remains unfolded.

of the two. The shallow minimum at 222 nm indicates that very little folding and helical content occurs in the covalent c-Myc*/c-Myc* (Figure 5B, red). However, as described before (*24*), the covalent Max*/Max* displays a strong helical content (Figure 5B, blue). Interestingly, when the covalent c-Myc*/c-Myc* is mixed with Max*/Max*, the interaction between both dimers results in a dramatic increase in helical content. The minimum at 222 nm is much more negative than the arithmetic sum of both homodimers' signals. This can only be explained by the stabilization of c-Myc*/c-Myc* helical structure through interactions with Max*/Max* in a tetrameric state as depicted in Figure 5C. In Figure 5A, lane 6, where the mixture between c-Myc*/c-Myc* and Max*/Max* was incubated with E-box DNA, two bands can be distinguished, one with the molecular weight of Max*/Max*/E-box complex (lane 2) and another at a higher molecular weight. This band corresponds to the mandatory c-Myc*/Max* tetramer in complex with E-box DNA. For the sake of clarity the mandatory c-Myc*/Max* tetramer is referred to as tetramer* in the rest of the text. Taken altogether, these results clearly demonstrate that, in our conditions, the covalent and dissociable c-Myc*/Max* have molecular weights of dimeric rather than tetrameric protein complexes.

Binding of the Tetramer to phTERT.* An equimolar mixture between the covalent c-Myc*/c-Myc* and covalent Max*/Max* (tetramer*) was added to DNA, and the resulting complexes were imaged by AFM (Figure 7). The binding events recorded with the tetramer* were found to be specific, as in the case of the heterodimer. Figure 7F shows a histogram of the localization of the binding events ($N = 147$). The four expected binding signatures were recorded (see Table 1). However, an additional signature emerges, i.e., the formation of several specific loops (in Figure 7A and collapsed loop in Figure 7B) and cross-linking events (Figure 7D). Moreover, the binding of the tetramer* engendered a shorter population of the promoter (538 ± 8 nm (L'), Figure 7E) compared to the full length population (614 ± 11 nm (L)). As expected, this length difference ($L - L'$) corresponds to the length of a loop (208 bp or 71 nm, see Figure 3 and

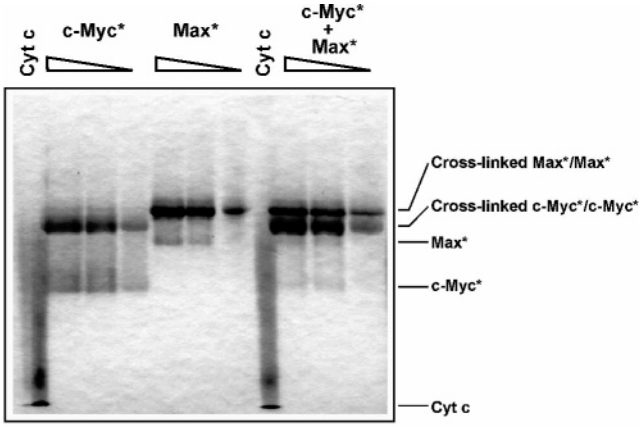

FIGURE 6: Electrophoretic mobility of the cross-linked c-Myc*/c-Myc* and Max*/Max* at different concentrations measured by cationic PAGE (in the absence of SDS) in the presence of 6 M urea at pH 7.00. The electrophoresis was performed in reverse polarity. The cross-linked c-Myc*/c-Myc* is observed to have a larger electrophoretic mobility than the cross-linked Max*/Max* dimer by virtue of its larger charge/mass ratio (1.10×10^{-22} C/g vs 7.08×10^{-23} C/g at pH 7.00). Cytochrome *C* (Cyt-C) is used as a marker.

Table 1). Here, the length measurements were done following the shortest path from one end to the other end of the promoters and omitting any discontinuity along the measuring path. It should be noted that a large number of loops appeared collapsed in our AFM images (Figure 7B,C). It is fascinating to relate that some double cross-link (Figure 7D) could be imaged. Indeed, considering that a promoter can be modeled as a rod made of 31 segments of 20 nm, it is very unlikely that four E-box sites from two promoters can come in contact randomly. The probability for this event can be estimated to $1/31^4$. This strongly advocates for a highly specific protein/DNA interaction mediated by two tetramers*. Altogether, these results indicate that loops can be induced by an artificial tetramer and imaged by AFM. Because no loops were found at this range of concentration with the c-Myc*/Max* dimer, this also signifies that if the dimer of dimers proposed by Nair and Burley (*10*) exists, then the interaction between the E-box and each dimer is stronger than the proposed interaction between dimers to form a tetramer. Hence we speculate that this dimer−dimer interaction is not strong enough to sustain the entropic cost associated with loop formation.

Imaging of the Max/Max* on phTERT.* Because the covalent Max*/Max* is also present with the tetramer*, one could argue that the various features (loop and/or cross-links of DNA strands) seen were caused by the Max*/Max* species. In order to rule out such a possibility, the binding of the dissociable Max homodimer to phTERT was imaged. Once again, the length of the DNA substrate (Table 1) was unaffected by the binding of the proteins ($N = 69$), and the repartition of the binding events was similar to that of the heterodimer, with peaks fitted close to the expected values (Table 1) and no occurrence of specific cross-links or loops.

CONCLUSION

We report the direct visualization of the specific binding of the dimeric Max/Max and c-Myc/Max b-HLH-LZ to the two E-box sequences of the hTERT promoter by AFM. In contradiction with a recent hypothesis, the heterodimeric

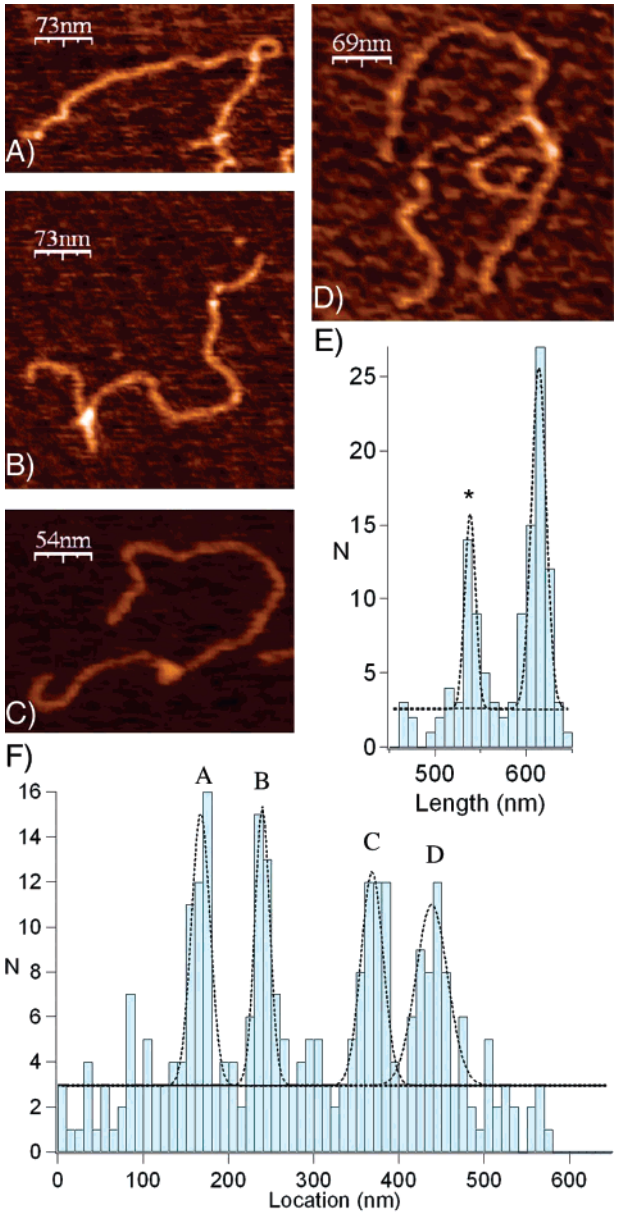

FIGURE 7: Binding of the mandatory c-Myc*/Max* heterotetramer to E-boxes on phTERT. Images of a DNA strand bound by the tetramer* (A) causing a loop or (B, C) causing a collapsed loop. (D) A bivalent structure caused by specific interactions between each E-box of each promoter. (E) DNA length of phTERT strands bound by the heterotetramer. The asterisk marks a shorter population specific to experiments using the tetramer*. (F) Position of the tetramer* on the phTERT fragment. Each peak corresponds to a theoretical position labeled from A to D (see Figure 3). Gaussian fitting results are reported in Table 1. The four Gaussian fits superimpose at their baseline which correspond to the occurrence of unspecific binding events.

c-Myc/Max b-HLH-LZ was not observed to form a dimer of dimers and to loop the phTERT promoter. While we cannot totally exclude that a population of a head-to-tail dimer of the c-Myc/Max b-HLH-LZ exists in solution, we suggest that the interactions responsible for the proposed tetrameric form are too weak to support the entropic cost of maintaining two E-box sequences close together in space. However using a designed and mandatory heterotetrameric c-Myc/Max b-HLH-LZ, it was possible to induce and observe by AFM the formation of loops in the hTERT promoter. It can therefore be assumed that the binding strength between

the two b-HLH domains of the mandatory tetramer and the E-box sequences is large enough to allow for the formation of complex topological states in DNA strands containing several E-box sites—that is for sustaining DNA looping or cross-linking. Overall, our results argue against the induction of complex DNA topologies by a heterotetramer of c-Myc/Max *in vivo*. Interestingly, the binding of the c-Myc/Max b-HLH-LZ was found to induce a bending of the phTERT strand. This bending could facilitate the binding of other proteins involved in transcription regulation (*1*). Moreover, *in vivo* Myc binding was shown to be preferentially located to euchromatic islands and to depend on specific histone marks (*32*). This suggests that Myc could participate in the structural maintenance of nucleosomes by its effect on the curvature of DNA. Finally, we found that the accuracy in DNA binding site localization of our experiments is approximately 20 bp and that E-box sites are specifically recognized and with equal apparent affinity (based on similar binding probability observed in the histogram) of the protein complexes for the phTERT promoter. This establishes our AFM protocol as a valuable method for the identification of binding sites for transcription factors whose cognate DNA binding sequence is unknown, and to explore the peculiar topological changes induced by the binding of a transcription factor.

REFERENCES

1. Semsey, S., Virnik, K., and Adhya, S. (2005) A gamut of loops: Meandering DNA, *Trends Biochem. Sci. 30*, 334−341.
2. Vilar, J. M., and Saiz, L. (2005) DNA looping in gene regulation: From the assembly of macromolecular complexes to the control of transcriptional noise, *Curr. Opin. Genet. Dev. 15*, 136−144.
3. Cole, M. D., and Nikiforov, M. A. (2006) Transcriptional activation by the Myc oncoprotein, *Curr. Top. Microbiol. Immunol. 302*, 33−50.
4. Rottmann, S., and Luscher, B. (2006) The mad side of the max network: Antagonizing the function of myc and more, *Curr. Top. Microbiol. Immunol. 302*, 63−122.
5. Blackwood, E. M., and Eisenman, R. N. (1991) Max: A helix-loop-helix zipper protein that forms a sequence-specific DNA-binding complex with myc, *Science 251*, 1211−1217.
6. Naud, J. F., McDuff, F. O., Sauve, S., Montagne, M., Webb, B. A., Smith, S. P., Chabot, B., and Lavigne, P. (2005) Structural and thermodynamical characterization of the complete p21 gene product of max, *Biochemistry 44*, 12746−12758.
7. Sauve, S., Tremblay, L., and Lavigne, P. (2004) The NMR solution structure of a mutant of the max b/HLH/LZ free of DNA: Insights into the specific and reversible DNA binding mechanism of dimeric transcription factors, *J. Mol. Biol. 342*, 813−832.
8. Brownlie, P., Ceska, T., Lamers, M., Romier, C., Stier, G., Teo, H., and Suck, D. (1997) The crystal structure of an intact human max-DNA complex: New insights into mechanisms of transcriptional control, *Structure 5*, 509−520.
9. Ferre-D'Amare, A. R., Prendergast, G. C., Ziff, E. B., and Burley, S. K. (1993) Recognition by max of its cognate DNA through a dimeric b/HLH/Z domain, *Nature 363*, 38−45.
10. Nair, S. K., and Burley, S. K. (2003) X-ray structures of myc-max and mad-max recognizing DNA. molecular bases of regulation by proto-oncogenic transcription factors, *Cell 112*, 193−205.
11. Lysetska, M., Zettl, H., Oka, I., Lipps, G., Krauss, G., and Krausch, G. (2005) Site-specific binding of the 9.5 kilodalton DNA-binding protein ORF80 visualized by atomic force microscopy, *Biomacromolecules 6*, 1252−1257.
12. Yang, Y., Sass, L. E., Du, C., Hsieh, P., and Erie, D. A. (2005) Determination of protein-DNA binding constants and specificities from statistical analyses of single molecules: MutS-DNA interactions, *Nucleic Acids Res. 33*, 4322−4334.
13. Berge, T., Ellis, D. J., Dryden, D. T., Edwardson, J. M., and Henderson, R. M. (2000) Translocation-independent dimerization of the EcoKI endonuclease visualized by atomic force microscopy, *Biophys. J. 79*, 479−484.
14. Kasas, S., Thomson, N. H., Smith, B. L., Hansma, H. G., Zhu, X., Guthold, M., Bustamante, C., Kool, E. T., Kashlev, M., and Hansma, P. K. (1997) Escherichia coli RNA polymerase activity observed using atomic force microscopy, *Biochemistry 36*, 461−468.
15. Rivetti, C., Guthold, M., and Bustamante, C. (1999) Wrapping of DNA around the E. coli RNA polymerase open promoter complex, *EMBO J. 18*, 4464−4475.
16. Guthold, M., Zhu, X., Rivetti, C., Yang, G., Thomson, N. H., Kasas, S., Hansma, H. G., Smith, B., Hansma, P. K., and Bustamante, C. (1999) Direct observation of one-dimensional diffusion and transcription by escherichia coli RNA polymerase, *Biophys. J. 77*, 2284−2294.
17. Sattin, B. D., and Goh, M. C. (2004) Direct observation of the assembly of RecA/DNA complexes by atomic force microscopy, *Biophys. J. 87*, 3430−3436.
18. Reich, S., Gossl, I., Reuter, M., Rabe, J. P., and Kruger, D. H. (2004) Scanning force microscopy of DNA translocation by the type III restriction enzyme EcoP15I, *J. Mol. Biol. 341*, 337−343.
19. Moreno-Herrero, F., Herrero, P., Colchero, J., Baro, A. M., and Moreno, F. (2001) Imaging and mapping protein-binding sites on DNA regulatory regions with atomic force microscopy, *Biochem. Biophys. Res. Commun. 280*, 151−157.
20. Ogata, K., Sato, K., and Tahirov, T. H. (2003) Eukaryotic transcriptional regulatory complexes: Cooperativity from near and afar, *Curr. Opin. Struct. Biol. 13*, 40−48.
21. Zhou, H., Zhang, Y., Ou-Yang, Z., Lindsay, S. M., Feng, X. Z., Balagurumoorthy, P., and Harrington, R. E. (2001) Conformation and rigidity of DNA microcircles containing waf1 response element for p53 regulatory protein, *J. Mol. Biol. 306*, 227−238.
22. Solis, F. J., Bash, R., Yodh, J., Lindsay, S. M., and Lohr, D. (2004) A statistical thermodynamic model applied to experimental AFM population and location data is able to quantify DNA-histone binding strength and internucleosomal interaction differences between acetylated and unacetylated nucleosomal arrays, *Biophys. J. 87*, 3372−3387.
23. Cong, Y. S., Wen, J., and Bacchetti, S. (1999) The human telomerase catalytic subunit hTERT: Organization of the gene and characterization of the promoter, *Hum. Mol. Genet. 8*, 137−142.
24. Jean-Francois, N., Frederic, G., Raymund, W., Benoit, C., and Lavigne, P. (2003) Improving the thermodynamic stability of the leucine zipper of max increases the stability of its b-HLH-LZ:E-box complex, *J. Mol. Biol. 326*, 1577−1595.
25. Hu, J., Banerjee, A., and Goss, D. J. (2005) Assembly of b/HLH/z proteins c-myc, max, and Mad1 with cognate DNA: Importance of protein-protein and protein-DNA interactions, *Biochemistry 44*, 11855−11863.
26. Fieber, W., Schneider, M. L., Matt, T., Krautler, B., Konrat, R., and Bister, K. (2001) Structure, function, and dynamics of the dimerization and DNA-binding domain of oncogenic transcription factor v-myc, *J. Mol. Biol. 307*, 1395−1410.
27. Krylov, D., Kasai, K., Echlin, D. R., Taparowsky, E. J., Arnheiter, H., and Vinson, C. (1997) A general method to design dominant negatives to B-HLHZip proteins that abolish DNA binding, *Proc. Natl. Acad. Sci. U.S.A. 94*, 12274−12279.
28. Chrambach, A., and Jovin, T. M. (1983) Selected buffer systems for moving boundary electrophoresis on gels at various pH values, presented in a simplified manner, *Electrophoresis 4*, 190−204.
29. Kholer, J. J., Metallo, S. J., Schneider, T. L., and Schepartz, A. (1999) DNA specificity enchanced by sequential binding of protein monomers, *Proc. Natl. Acad. Sci. U.S.A. 96*, 11735−11739
30. Dahlgren, P. R., and Lyubchenko, Y. L. (2002) Atomic force microscopy study of the effects of mg(2+) and other divalent cations on the end-to-end DNA interactions, *Biochemistry 41*, 11372−11378.
31. Fisher, D. E., Parent, L. A., and Sharp, P. A. (1992) Myc/Max and other helix-loop-helix/leucine zipper proteins bend DNA toward the minor groove, *Proc. Natl. Acad. Sci. U.S.A. 89*, 11779−11783.
32. Guccione, E., Martinato, F., Finocchiaro, G., Luzi, L., Tizzoni, L., Dal'Olio, V., Zardo, G., Nervi, C.; Bernard, L., and Amati, B. (2006) Myc-binding-site recognition in the human genome is determined by chromatin context, *Nat. Cell Biol. 8*, 764−770.

BI700076M